

COMPARATIVE ELEMENTAL ASSOCIATIONS IN LIGNITES
HAVING SIGNIFICANT WITHIN-MINE VARIABILITY OF SODIUM CONTENT

J.P. Hurley and S.A. Benson

University of North Dakota
Energy Research Center
Box 8213, University Station
Grand Forks, North Dakota 58202

Introduction

The inorganic constituents of lignites from the Fort Union Region are distributed within the coal matrix as cations, coordinated species and minerals (1). The quantities of inorganics present in these lignites have significant within-mine, or intramine, variability (2). Studies have indicated that high-sodium coals from this region cause severe ash fouling of heat exchange surfaces in utility boilers (3). The coals investigated were collected from pits within the Gascoyne Mine, Bowman County, North Dakota and Beulah Mine, Mercer County, North Dakota. From each mine, two samples were selected having significant differences in sodium content and different fouling characteristics in utility boilers.

The distribution of inorganics constituents within the Gascoyne and Beulah coals was determined by non-quantitative identification of mineral matter and by chemical fractionation to ascertain any significant differences in the association of elements within the coals. In addition, the amounts of ion exchangeable cations were related to the carboxylate content of the coals.

Experimental

Samples were collected according to a procedure used by Benson (4). Proximate and ultimate analyses were performed on the air-dried coals using standard ASTM methods (5). Bulk coal mineralogy was determined by x-ray diffraction (XRD) of the coal's low-temperature ash (LTA) (6) and by scanning electron microprobe (SEM) in conjunction with energy dispersive x-ray analysis (EDX) (7) of the coal. Carboxylate contents were determined by exchanging the demineralized coals (8) with 1M barium acetate, followed by potentiometric titration with 0.2N barium hydroxide to pH 8.25 to determine the acid produced (9). The determination of inorganic constituents of the starting coals and subsequent residues was performed by x-ray fluorescence (XRF) (10) and neutron activation analysis (NAA) (11). The chemical fractionation was done with a method modified from that of Miller and Given (1). Two samples of each coal were ground to less than approximately 325 mesh in an alumina grinder and freeze dried for two days. The dried coal was mixed with 100 ml of 1N ammonium acetate and stirred for 24 hours at 70°C in a plastic beaker. The mixture was filtered, the residue washed, and the extract made up to 250 ml. The dried residue was extracted two more times with ammonium acetate, then twice with 1N hydrochloric acid in the same manner. All of the extracts were analyzed with inductively coupled argon plasma spectrometry (ICAP). A portion of the residue left after the ammonium acetate extractions and a portion left after the hydrochloric acid extractions were analyzed by XRF and NAA.

Results and Discussion

Coal Compositions. Table I shows the initial elemental, proximate, ultimate, and carboxylate content analysis of the coals on a moisture free basis.

Table I. Dry Bulk Coal Elemental, Ultimate, Proximate, and Carboxylate Analyses

	Gascoyne Low Sodium	Gascoyne High Sodium	Beulah Low Sodium	Beulah High Sodium
Na ($\mu\text{g/g}$)	1317	2694	1379	4625
Mg ($\mu\text{g/g}$)	2991	2588	1476	979
Al ($\mu\text{g/g}$)	8740	7300	5420	2890
Si ($\mu\text{g/g}$)	28640	10920	8950	3530
K ($\mu\text{g/g}$)	1260	1430	916	ND*
Ca ($\mu\text{g/g}$)	17370	22790	15610	18110
Ti ($\mu\text{g/g}$)	1180	546	503	583
Mn ($\mu\text{g/g}$)	123	163	52	24
Fe ($\mu\text{g/g}$)	3890	2540	10240	5160
Ba ($\mu\text{g/g}$)	593	1268	179	397
C (wt %)	58.3	54.5	61.4	66.4
H (wt %)	4.0	5.2	4.1	3.6
N (wt %)	0.88	0.84	0.42	0.87
S (wt %)	1.7	1.4	3.2	1.2
O (diff.)	19.6	29.3	18.2	19.5
Ash (wt %)	15.5	8.8	12.6	8.4
Carboxylate groups (meq/g)	2.46	2.54	2.47	2.76

*ND - Not determined.

Similarities can be seen between the high-sodium coals versus their intramine low-sodium counterparts. In the high-sodium coals, the carboxylate, calcium, and barium contents are greater. Magnesium, aluminum, silicon, iron, and ash contents are lower in the high-sodium coals than in their intramine low-sodium counterparts.

Coal Mineralogy. The mineralogies of the coals, determined by x-ray diffraction of their low-temperature ashes, are similar. The diffractogram shown in Figure 1 is of the LTA of the Gascoyne high sodium coal. The mineral phases which were in sufficient amounts (2-5% depending on crystal structure) to be clearly delineated include quartz (SiO_2), micaceous clay minerals, and pyrite (FeS_2). Some bassanite ($\text{CaSO}_4 \cdot 1/2 \text{H}_2\text{O}$) was identified in the LTA of the Beulah coals although it is not clear if this forms from sulfur fixation during ashing (12) or from the dehydration of gypsum. The quartz peaks are more prominent in the diffractograms of the ash from the low-sodium (high-ash) coals.

In addition to the minerals mentioned above, the SEM-EDX work showed minor amounts of dolomite ($\text{CaMg}(\text{CO}_3)_2$), calcite (CaCO_3), gypsum

(CaSO₄·2H₂O), rutile (TiO₂), hematite (Fe₂O₃) (7), and barite (BaSO₄) (7). Also, the micaceous clay minerals identified by XRD were seen to include kaolinite, illites, and micas. Most of the SEM-EDX work was not systematic so quantitative comparisons between the coals will not be made here.

Ammonium Acetate Treatments. The percentages of the elements removed from the coals by the ammonium acetate treatments are shown in Table II. The figures for the carboxylate ions are percentages of the carboxyl groups that are in a salt form, under the assumption that all of the cations removed by the ammonium acetate treatments were exchanged from these sites. Minor amounts of these elements may have been exchanged from other organic acids or micaceous clays, or may have come from the dissolution of minerals soluble in ammonium acetate such as gypsum, calcite, and dolomite.

Table II. Elements Removed by Ammonium Acetate (%)

	Gascoyne Low Sodium	Gascoyne High Sodium	Beulah Low Sodium	Beulah High Sodium
Na	100	100	100	100
Mg	74	75	76	84
Al	0	0	0	0
Si	0	1	0	0
K	22	19	7	*31
Ca	78	85	82	77
Ti	0	0	0	0
Mn	34	39	25	21
Fe	0	0	0	0
Ba	39	61	72	88
Carboxyl groups (% in salt form)	38	51	32	35

*ppm removed

The results indicate aluminum, silicon, titanium, and iron are not removed from any of the coals by this treatment. Among those elements that are extracted, a higher percentage of barium is removed from the high-sodium coals than from their intramine low-sodium counterparts. However, more barium is removed by each of the second and third treatments than by the first so we feel that the barium extraction was incomplete. A large percentage of the sodium, calcium, and magnesium was removed from all of the coals.

Hydrochloric Acid Treatments. Table III lists the percentage of elements removed by the hydrochloric acid treatments. The elements removed by this treatment were associated with the coal as oxides, carbonates, coordinated complexes within the coal organic structure and certain elements (Mg, Al, Si, K, Ca, Fe) which can be extracted from the micaceous clay minerals.

A higher percentage of aluminum was removed from the high-sodium (low-ash) coals than from the corresponding intramine low-sodium

Table III. Elements Removed by Hydrochloric Acid (%)

	Gascoyne Low Sodium	Gascoyne High Sodium	Beulah Low Sodium	Beulah High Sodium
Na	0	0	0	0
Mg	12	16	17	16
Al	42	51	60	80
Si	3	12	14	12
K	30	41	19	*206
Ca	20	14	17	22
Ti	4	7	5	2
Mn	64	60	69	76
Fe	73	68	37	42
Ba	43	39	16	12

*ppm removed

(high-ash) coals. Although more aluminum was actually removed from the low-sodium coals, we feel that the solutions were not saturated because much lower levels of aluminum were found in the second extracts than in the first. Instead, we believe that the higher relative removal from the high-sodium coals is due to differences in the types of micaceous clay minerals present. In all the coals the ratio of aluminum to silicon removed (4:1 - 14:1) does not match the ratios found in common micaceous clay minerals. This indicates that the micaceous clays have not dissolved but that a selective attack has occurred on the gibbsite (aluminum containing) layer in the micaceous clays.

Insolubles. Table IV shows the elemental percentages left in the residue after the chemical fractionation process.

Little or no sodium, magnesium, calcium, and manganese remain in the coals. X-ray diffraction of the low temperature ash of the residue from the Gascoyne high-sodium coal shows that the major remaining minerals are the same as those seen in the LTA of the bulk coal; i.e., quartz (SiO_2), micaceous clays, and pyrite (FeS_2). Work done with the SEM-EDX suggests that the potassium remaining in the residue is found in the micaceous clays, titanium in a rutile form (TiO_2), and the barium present as barite (BaSO_4)(7). It is interesting that no barium is left in the high-sodium coals even though they originally contained more barium than the low-sodium coals.

Conclusions

The amount and mode of occurrence of inorganics in lignites can have a pronounced effect on the efficiency of the coal's utilization. This study used a number of the techniques developed by others to investigate variations in the inorganic makeup of coals found in two areas within each of two mines. By better understanding these

Table IV. Elements Remaining After All Treatments (%)

	Gascoyne Low Sodium	Gascoyne High Sodium	Beulah Low Sodium	Beulah High Sodium
Na	0	0	0	0
Mg	14	9	7	0
Al	58	49	40	20
Si	97	87	86	88
K	48	40	74	*ND
Ca	2	1	1	1
Ti	96	93	95	98
Mn	2	1	6	3
Fe	27	32	63	58
Ba	18	0	12	0

*Not determined.

variations, insights into the various depositional and post depositional processes may be gained. Also, understanding the modes of occurrence of the inorganic constituents of a coal may help in determining its appropriate utilization.

A comparison of the elemental associations between the high-sodium coals and their intramine low-sodium counterparts shows:

1. No significant differences in the modes of occurrence of the inorganic constituents exist, only differences in the amounts of inorganic species.
2. A higher percentage of aluminum is extracted from the high-sodium coals indicating different types of predominant micaceous clay minerals.
3. A higher percentage of barium is associated with ion exchange sites in the high-sodium coals.

Further work needs to be done in determining the exact mineralogic makeup and types of organic acids found in the coals, as well as accumulating more data from which to draw further conclusions.

Literature Cited

1. Miller, R.N.; and Given, P.H. A Geochemical Study of the Inorganic Constituents in Some Low-Rank Coals. U.S. DOE Report, FE-2494-TR-1, February 1978.
2. Cooley, S.A.; and Ellman, R.C., Analysis of the Northern Great Plains Province Lignites and Subbituminous Coals and Their Ash, DOE/GFETC/RI-81/2, DE81028366, July 1981.
3. Sondreal, E.A.; Tufte, P.H.; Beckering, W. Ash Fouling in Combustion of Low-Rank Western U.S. Coals, Combustion Science and Technology, Vo. 16, pp. 95-110, 1977.
4. Benson, S.A.; Kleesattel, D.R.; and Schobert, H.H. ACS Division of Fuel Chemistry Preprints 1984, 29, (1), 108.
5. "Annual Book of ASTM Standards" 1983, 05.05, D3172-73; D3176-74.
6. Miller, R.N.; Yarzab, R.F.; and Given, P.H. Fuel, 1979, 58, 4.

7. Zygarlicke, C.J. 'The Occurrence and Distribution of Inorganic Constituents in a North Dakota Lignite: an SEM and Statistical Analysis Approach'. Internal Report, University of North Dakota Energy Research Center, UNDERC-IR-6, 1983.
8. Tarpley, E.C.; and Ode, W.H. 'Evaluation of an Acid-Extraction Method for Determining Mineral Matter in American Coals'. Report of Investigations 5470, U.S. Department of the Interior, Bureau of Mines, 1959.
9. Schafer, H.N.S. Fuel, 1970, 49, 197.
10. Benson, S.A.; Severson, A.L.; and Beckering, W. Amer. Lab. 1980, 12(10), 35.
11. Weaver, J.N. in 'Analytical Methods for Coal and Coal Products, Vol. I' (Ed. C. Karr), Academic Press, New York, 1978, p. 377.
12. Painter, P.C.; Coleman, M.M.; Jenkins, R.G.; and Walker, P.L. Jr., Fuel 1978, 57, 125.

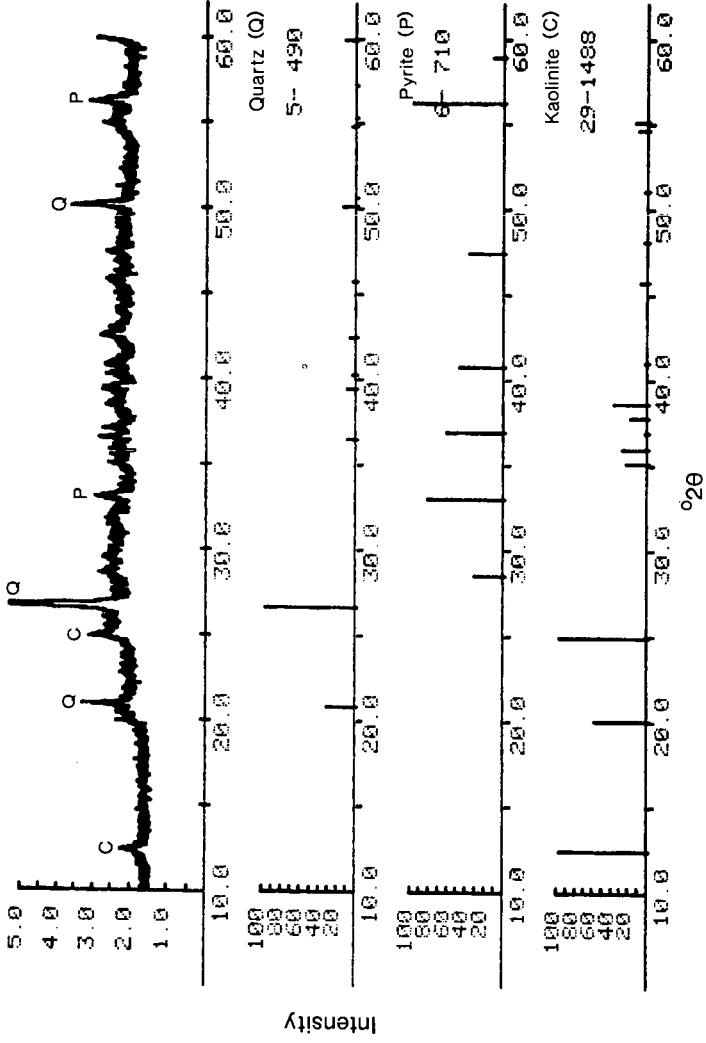


FIGURE 1. Diffractogram of the Gascoyne High-Sodium LTA along with reference graphs for quartz, pyrite, and kaolinite.

RUTHENIUM TETROXIDE OXIDATION OF LIGNITE

E.S. Olson and J.W. Diehl

University of North Dakota Energy Research Center
Box 8213, University Station
Grand Forks, North Dakota 58202

The objective of these studies was to develop new methods for the elucidation of the organic structure of low-rank coals, especially with regard to the nature of the hydroaromatic groups, the substituent groups on aromatic moieties and bridging groups between aromatic moieties. Isolation of the nonaromatic groups in coal could be achieved if the aromatic rings in the structure could be oxidized without degrading the alkyl substituents on the aromatic rings. Selective oxidation of the benzene ring has been observed in reactions with trifluoroperacetic acid (1); however the severe conditions required with this reagent result in extensive degradation of the alkyl groups (2). Thus tetralin gave succinic, glutaric, and adipic acids in the ratio 1:4:4(3). Confusion also resulted from the isolation of different products when different acid concentrations were used in the oxidation, e.g. cyclohexene-1,2-dicarboxylic anhydride was reported as the product from tetralin (1).

Ruthenium tetroxide is a useful reagent for the oxidation of alcohols, ethers, aldehydes, amides, alkenes and aromatic compounds (4). In the case of alkylbenzenes, the benzene ring is preferentially attacked, preserving any alkyl substituents as aliphatic carboxylic acids. Stock has reported the oxidation of Illinois No. 6 coal (5) using ruthenium tetroxide in a coordinating cosolvent, acetonitrile, which enabled the oxidation to proceed with much higher conversions (6).

We have reported the use of the ruthenium tetroxide with a phase transfer catalyst, a quaternary ammonium salt, in a carbon tetrachloride-aqueous system for the analysis of alkylnaphthalenes and a North Dakota lignite sample (3). The phase transfer catalyst transports the primary oxidant (periodate) into the organic phase as well as removes the carboxylate products from the organic phase. Improvement of the yield is believed to result from the avoidance of an inactive complex formed by the acid products with the ruthenium tetroxide. This method was used previously for the synthesis of fatty acids from 1-alkenes (7).

A number of model compounds were oxidized with ruthenium tetroxide in the two-phase system so that the method could be evaluated and compared with ruthenium tetroxide oxidation in acetonitrile. Reactions were carried out as reported earlier (3). Methods which did not require derivatization were devised for the analysis of the reaction products. The aqueous layer was analyzed on an ion moderated reverse phase HPLC column (Aminex HPX-87H) using 0.008 N H_2SO_4 as the eluent (1 ml/min) (refractive index detection). 3-Methyladipic acid was added as an internal standard and the system was calibrated for malonic, succinic, glutaric, adipic, and phthalic acids (single level calibration). The aqueous layer was also analyzed by GC with an AT-1000 phase fused silica capillary column. This column was calibrated for benzoic, phenylacetic and hydrocinnamic acids using 2-methylbutyric acid as the internal standard (multilevel calibration). The carbon tetrachloride layer was analyzed on an SE54 fused silica column calibrated for the aromatics, hydroaromatics and ketones and on the AT1000 column for the same acids as above. Diphenic acid was extracted from the carbon tetrachloride layer with NaOH and analyzed by weighing the crystals obtained after acidification of the extract.

High conversions were observed for the model compounds oxidized with RuO_4 in the two-phase system with a phase transfer catalyst (Table I). The conversions for diphenylmethane and bibenzyl were a little higher than when acetonitrile was used as the solvent. Another indication of higher reactivity for ruthenium tetroxide in the

Table I. Oxidation of Model Compounds With Ruthenium Tetroxide and Phase Transfer Catalyst (PT cat.)

Compound	Conversion	Product	Product Distribution	
			PT Cat.	Acetonitrile ^a
Indan	100%	1-Indanone	31	16
		Glutaric Acid	64	77
		Succinic Acid	5	7
Tetralin	100%	1-Tetralone	26	8
		Adipic Acid	50	75
		Glutaric Acid	24	17
Diphenylmethane	80%	Benzophenone	18	32
		Phenylacetic Acid	70	41
		Benzoic Acid	12	4
Bibenzyl	90%	Benzil	1	Trace
		Succinic Acid	43	35
		Hydrocinnamic Acid	45	63
		Phenylacetic Acid	2	--
		Benzoic Acid	10	--
Phenanthrene	100%	Phenanthrenequinone	2	4
		Diphenic Acid	92	91
		Phthalic Acid	6	5

^a = Data from reference 5.

two-phase system over the acetonitrile system is the greater yield of succinic acid as compared with hydrocinnamic acid in the oxidation of bibenzyl.

Oxidation of the alkyl substituent groups at the α -carbon to give the aryl ketone occurred in all model compounds. This was observed to a greater extent with indan and tetralin and to a lesser extent with diphenylmethane, as compared to the oxidation carried out with acetonitrile cosolvent. The ratio of glutaric to succinic acids resulting from the oxidation of indan was greater than 10 to 1 for both oxidation conditions. The ratio of adipic to glutaric acids from the oxidation of tetralin was higher when acetonitrile was used. The selectivity of the ruthenium tetroxide reagent for aryl versus alkyl attack thus varies in the two methods with the type of substrate being oxidized. Oxidation of the PAH, phenanthrene, showed no difference in product distribution between the two systems.

The oxidation of lignite (Beulah mine) with ruthenium tetroxide proceeded rapidly at room temperature. The products from the oxidation in the aqueous layer could not be analyzed directly by the HPLC method because the solution was too dilute. Diazomethane in ether was stirred with the aqueous layer for two hours to convert the acids to ether soluble esters, which were analyzed by GC (DB1701 capillary column) (see Figure 1). Table II lists major components and the relative GC peak area percentages.

The major components were aliphatic dicarboxylic acids and benzene polycarboxylic acids. Very low concentrations of aliphatic monocarboxylic acids were formed. Since succinic acid is present in the largest concentrations of the diacids, we may infer that a major structural feature of the lignite is a

TABLE II
 CARBOXYLIC ACIDS FROM RuO₄ OXIDATION OF BEULAH LIGNITE (See Figure 1)

Peak No.	Compound (as methyl ester)	Area, %
1	siccinic	10.7
2	methylsuccinic	1.1
3	glutaric	7.6
4	methyl glutaric	1.0
5	adipic	2.7
6	unknown	7.7
7	phthalic	0.7
8	terephthalic	0.4
9	isophthalic	0.2
10	unknown	3.2
11	benzene-1,2,4-tricarboxylic	3.4
12	benzene-1,2,3-tricarboxylic	4.2
13	benzene-1,3,5-tricarboxylic	0.7
14	benzene-1,2,4,5-tetracarboxylic	5.7
15	benzene-1,2,3,4-tetracarboxylic	4.5
16	benzene-1,2,3,5-tetracarboxylic	5.7
17	benzene pentacarboxylic	7.3

dimethylene bridge occurring between aromatic moieties or present in a hydroaromatic such as 4,5-dihdropyrene. The model compound studies with diphenylmethane show that this method is limited in its applicability to the determination of single methylene bridges. Since malonic acid was produced in only trace amounts from oxidation of diphenylmethane, the absence of malonic acid in the lignite oxidation products does not rule out methylene bridges between aromatics in the coal.

The greater amounts of benzenepolycarboxylic acids relative to the benzenedicarboxylic acids which would be expected from naphthalene oxidation may seem surprising, however some of the acid groups were undoubtedly present in the coal before the oxidation. This aspect is being studied by labeling the original acid groups.

In order to fully interpret the results of the lignite oxidation with this reagent, the oxidation of several more model compounds will be studied. Quantitation of the methyl esters of the products from the lignite oxidation is also in progress.

Literature Cited

1. Deno, N.C.; Greigger, B.A.; and Stroud, S.G., Fuel (1978) 57, 455.
2. Liotta, R.; and Hoff, W.S., J. Org. Chem. (1980) 45, 2887; Hessley, R.K.; Benjamin, B.M.; and Larsen, J.W., Fuel (1982) 61, 1085.
3. Olson, E.S.; and Farnum, B.W. Amer. Chem. Soc., Div. Fuel Chem. Preprints (1981) 26, no. 1, 60.
4. Lee, D.G.; and van den Engh, M. in Oxidation in Organic Chemistry, Part B, W.S. Trahanovsky, ed., Academic, 177 (1973).
5. Stock, L.M.; and Tse, K.-t., Fuel (1983) 62, 974.

6. Carlsen, P.H.J.; Katsuki, T.; Martin, V.S.; and Sharpless, K.B., J. Org. Chem. (1981) 46, 3936.
7. Foglia, T.A.; Barr, P.A.; and Malloy, A.J., J. Amer. Oil Chemists' Soc. (1977) 54 858A.

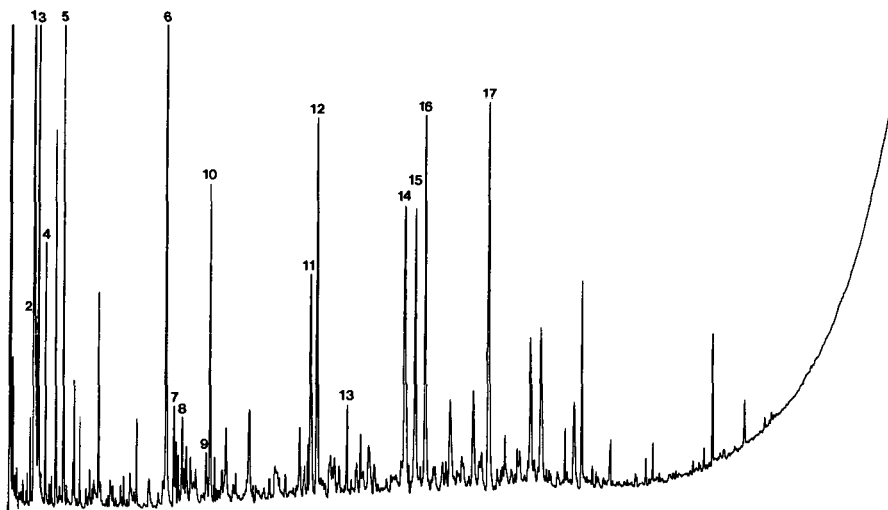


Figure 1. Methyl esters of products of ruthenium tetroxide oxidation of Beulah 3 lignite. DB1701 (0.25 μ) FSOT 15m x 0.32 mm. On-column injection. FID. H₂ carrier (41 cm/sec at 240°C).

FUEL NITROGEN EVOLUTION: COUPLING BETWEEN RANK AND HEATING CONDITIONS. J.F.Freihaut,
United Technologies Research Center, East Hartford, CT 06108.

A range of coals from a variety of geologic provinces have been devolatilized using both heated grid and flash lamp apparatus. Lignite, sub-bituminous, high, medium and low volatile bituminous and anthracite samples have been investigated. Final particle temperatures of 400 to 1500 C were obtained with the heated grid and heating rates approaching 10^6 C/sec in the flash lamp apparatus. In inert conditions and moderate heating rates (10^3 °C/sec or less) the evolution of fuel nitrogen mirrors, on a mass fraction basis, the evolution of parent coal as char, tar or light gas. The evolution of fuel nitrogen as a light gas is observed to be coupled to the fate of primary tars as they evolve. Thus the evolution of fuel nitrogen as a light gas during pyrolysis is observed to be rank dependent via the thermal stability characteristics of the primary tars.

Flash Pyrolysis of Cellulose in a Micro Fluidized Bed

T. Funazukuri, R.R. Hudgins and P.L. Silveston

Department of Chemical Engineering
University of Waterloo
Waterloo, Ontario, Canada N2L 3G1

INTRODUCTION

Short contact time or flash pyrolysis is one of the alternatives under consideration for the conversion of biomass into liquid or gaseous fuel, or perhaps into chemicals feedstock. A variety of compounds are formed in flash pyrolysis so that it would be desirable to be able to predict yields of at least the major products as a function of the pyrolysis device and operating conditions such as heating rate of the biomass, final temperature, particle size, gas phase composition. As a contribution to this goal, this paper considers the flash pyrolysis of micro crystalline cellulose powder and particles in a fluidized bed. By flash pyrolysis, we refer to heating rates (at the particle surface) greater than 100°C/s , final temperatures generally greater than 500°C and contact times of the order of 1-2 seconds or less. Compared with the vast literature on slow pyrolysis of cellulose the literature on flash pyrolysis is very small. A few studies have been made using a Pyroprobe or a Curie point pyrolyzer (Iglauer et al. (1974); Ohnishi et al., (1975) Hileman et al., (1979) and a fluidized bed (Barooah and Long, 1976); Maa and Bailie, (1978); Scott and Piskorz, (1981.) Irradiation was used by Martin (1965) and Shivadev and Emmons (1974) as a heat source. Lewellen et al. (1977) and Hajaligol et al. (1982) pyrolyzed filter paper suspended between two massive electrodes. The latter team succeeded in producing quite a wide range of temperatures and heating rates. Unfortunately, in most past studies, weight loss measurement and analysis of volatile products were not carried out simultaneously. Indeed, identification of volatile products usually came from investigations where the pyrolysis reactions went nearly to completion. In such cases, the product distribution might result from not only cellulose pyrolysis but also from secondary cracking and perhaps even char gasification.

EXPERIMENTAL SYSTEM, ANALYTICAL TECHNIQUES AND STUDY MATERIALS

Figure 1 shows the fluidized bed system used in this study. Details of the bed itself are given in Figure 2. The assembly shown in Figure 2 was built by Scott and Piskorz (1981) and used by them to study the flash pyrolysis of coal and wood.

Pyrolysis occurs in a bed of fluidized sand supported by a porous stainless steel distribution plate. The net reactor volume is 23 mL. Fluidizing gas is introduced from the bottom through a preheating tube 1 meter in length. As Figure 1 shows, the reactor sits in a three-zone Lindberg electric tube furnace, 91 cm in length. The reactor was located in the upper zone and the preheating tube of the reactor was situated in the bottom two zones and was sufficient to heat up the fluidizing gas to bed temperature before it entered the reactor.

The low rate of cellulose feed needed for the system was achieved using an entrainment feeder described by Scott and Piskorz (1981). Feed rate

could be adjusted from 5 to 100 g/h with this unit. Cellulose entrained in carrier gas entered the bed through the central, downwardly directed tube in Figure 2. The tip of this tube was immersed in the fluidized sand. The concentric tube, terminating in a 6.3 mm o.d. outlet was originally supposed to introduce a cold quench gas into the reactor. In this study, it served as sampling line to a Carle G.C. with a heated sampling loop. This G.C. periodically sampled the off gas and was used to insure the assembly operated at steady state.

Most of the volatile products and gas introduced to fluidize the sand bed and to entrain the cellulose feed left the reactor through the 12.7 mm o.d. outlet seen in Figure 2. This outlet was connected to the first of three, water-cooled glass condensers by about 40 cm of Teflon tubing. Almost all the tar formed and the char eluted from the bed was trapped in the condensers or in the connecting tubing. The remaining tar was caught in a glass-wool-filled column. After passing through two further columns to strip out water, the gas was collected in an inflatable bag.

A run using this equipment lasted about 30 minutes once steady state was established. Weighing provided the amount of cellulose fed to the fluidized bed and the char caught in the bed. Washing of the glass wool, tubing and condensers with ethanol provided a measure of the char eluted (by weighing the residue on filtering the solvent) and of the tar formed by weighing the residue after filtering and evaporating the solvent. GC analysis of the gas bag content and measurement of the gas volume gave the non-condensable, volatile products produced.

Analyses were performed using a dual channel GC equipped with a 1.83-m 100/120 mesh Porapak T column on one channel and a 1.83-m 80/100 mesh Porapak Q column in the other. Both channels used FID's and temperature programming was employed. A second chromatograph equipped with a 1.83-m mesh 5A molecular sieve column was also used on the gas bag to measure CO, CO₂ and water.

Tar samples were treated with N-trimethyl silylimidazole in pyridine. This reagent creates a volatilizable compound from levoglucosan; other tar compounds are also converted to volatilizable substances by silylation. Silylated tar solution was injected onto either a 1.83-m 6% OV-101 on 80/100 mesh Chromosorb column or a similar Chromosorb column treated with 6% SE-52. Peak identification was by means of pure levoglucosan dissolved in N-trimethyl silylimidazole.

A microcrystalline cellulose (MCP) furnished as a 200/270 mesh powder was the primary test material. Cellulose particles, as a 20/40 mesh material were made by pelletizing the MCP in a press, crushing the pellets, and then sieving. The particles permitted a test of a particle size on product distribution and pyrolysis rate to be made. Limitations of attainable fluidization velocity limited the size to 20/40 mesh.

Cellulose conversion and product distribution were measured at fluidized bed temperatures between 310 and 770°C. Most experiments were performed in an N₂ atmosphere, but measurements were made as well with CO, CO₂ and a H₂-N₂ mixture as the fluidizing gas. Contact time of cellulose in the bed was not less than 0.5 s (the residence time of the fluidizing gas in the bed), and probably did not exceed 2 to 3 seconds. Based on work with coal,

Tyler (1979) estimates that the heating rate of fine particles in a fluidized bed must be greater than 1°C/ms.

EXPERIMENTAL RESULTS

CO, CO₂ and H₂ pyrolysis yields from cellulose powder are shown in Figure 3. The carbon oxides are the major products. H₂ yields are the same order of magnitude as the hydrocarbon yields. A transition in behaviour occurs around 500°C. Above this temperature the CO yields increase at slower rate but the CO₂ yields level off. Char yields were less than 10 wt% of the sample fed above 500°C so that pyrolysis is essentially complete. The abrupt change in the CO₂ yield reflects, evidently, completion of the cracking reaction.

Yields of light hydrocarbon by carbon number vs temperature appear in Figure 4. A change in slope at about 500°C is evident. With the exception of flattening of the C₃ and C₄ yields above 700°C, the light hydrocarbon behaviour resembles the yield behaviour seen for CO. Probably cracking of C₃⁺ hydrocarbons at 700°C⁺ accounts for the flattening observation.

The major liquid oxygen-bearing molecules detected were acetaldehyde, acrolein, furan and acetone. While Hajaligol et al. (1982) measured relatively high methanol yields, 1 wt% of the pure cellulose sample, the yields in this study were as low as 0.1 wt% of the sample. Figure 5 shows yields of acetaldehyde while Figure 6 shows those of acetone plotted versus temperature. Data for MCP powder and 20/40 mesh pellets are plotted together. Particle size quite clearly does not affect yield. Measurements taken in different atmospheres are also shown. Once again, the atmosphere surrounding the pyrolyzing material does not change the yield temperature behaviour. Both these observations apply to the CO, CO₂ and H₂ yields and for the light hydrocarbons.

Acetaldehyde yield data (Figure 5) resembles that for CO, while the acetone yields are much more like the data obtained for CO₂ (Figure 3). Indeed, of the other two oxygen containing hydrocarbon which could be accurately measured, acrolein and furan, the former exhibited the CO behaviour with temperature while the latter appeared to show the CO₂ behaviour.

The yields of levoglucosan are shown in Figure 7. Particle size and fluidizing atmosphere do not affect the yields. Replotting the data against weight loss of the original MCP or cellulose particles permits a comparison with the yields data obtained by other workers for slow pyrolysis. Figure 8 provides the comparison. Yields found in this study were smaller by a factor of 2 to 3 than yields measured under slow pyrolysis. It is surprising that the agreement among the data of different investigators is so poor.

The difference between our data and others shown in Figure 8 is that heating and contact times in our study were perhaps an order of magnitude greater than those used by the others. If levoglucosan is a primary product of cellulose pyrolysis, as has been proposed, shorter contact times should increase not decrease yields. Evidently, at high temperatures, some of the cellulose molecules can be directly decomposed into smaller weight fragments and these free radicals can combine to form volatile products. Levoglucosan would not be formed as an intermediate for this route to the lower molecular weight products. This may be the explanation for the deviation of our data from those

obtained by Tsuchiya and Somi (1970) and some of the data of Shafizadeh et al. (1978a, 1979b).

Closure of the material balances to about 2% when MCP was pyrolyzed, permits a reliable picture to be drawn of the product distribution between solid tar, liquid and gas for flash pyrolysis in a fluidized bed. This distribution is shown as a function of temperature in Figure 9. Pyrolysis atmosphere and the particle size of cellulose up to 20 to 40 mesh do not affect the distributions. The levoglucosan product is also shown.

It is clear from the figure that the liquid-tar fraction of the products can be maximized by operating between 450 and 650°C. Higher temperatures increase gas production while lower temperatures result in large char residues.

The remarkably similar yield vs. temperature behavior seen in Figures 3 to 6 suggest cross plotting of the yield data. When this is done it is found that all the pyrolysis products with the exception of levoglucosan and other tar components plot as simple logarithmic functions of the form

$$Y_x = a Y_{CO}^b \quad (1)$$

against CO yield (Y_{CO}) or against CO_2 yield. Examples of such plots appear in figures 10 and 11. The functions are independent of temperature, gas atmosphere, and particle size. Linear relationships on these log-log plots hold very closely from CO yields of from 0.5 to 20 weight percent. Data of other studies, including Tsuchiya and Sumi (1970) who worked with slow pyrolysis, also give linear cross plots and both for furan and the light hydrocarbons these data agree quite well with what was observed in this study even though the pyrolysis technique differed substantially. Probably then, Equation 1 and its parameters are independent of the type of flash pyrolysis unit. Agreement was poorer for other products so probably Equation 1 cannot be generalized to slow pyrolysis. Yield relationships appear to offer a useful means of predicting product distribution in flash pyrolysis operations. The relationships are developed and discussed in more detail in a recent paper by Funazukuri et al. (1984).

REFERENCES

- Barooah, J.N., and Long, V.D., (1976) "Rates of thermal decomposition of some carbonaceous materials in a fluidized bed", *Fuel*, 55, 116-120.
- Funazukuri, T., Hudgins, R.R. and Silveston, P.L., (1984) "Prediction of Volatile Products from Thermal Conversion of Cellulose by Correlation with Carbon Oxides in the Gas", Preprint I.G.T. Conference on Fuels from Biomass and Wastes, Lake Buena Vista, Florida (February).
- Graham, R., Bergougnou, M.A., Mok, L.K. and de Lasa, H.L., (1982) "Flash pyrolysis (ultraprolysis) of biomass using solid heat carriers", research paper presented at Fundamentals of Thermochemical Biomass Conversion: An International Conference, Boulder, Colorado, October.

Hajaligol, M.R., Howard, J.B., Longwell, J.P. and Peters, W.A., (1982), "Product compositions and kinetics for rapid pyrolysis of cellulose", I/EC Process Des. Dev., 21, 457-465.

Halpern, Y. and Patai, S., (1969) "Pyrolytic reactions of carbohydrates. Part V. Isothermal decomposition of cellulose in vacuo", Israel J. of chem., 7, 673-683.

Hileman, F.D., Wojcik, L.H., Futrell, J.H. and Einhorn, I.N., (1976) "Comparison of the thermal degradation products of α -cellulose and douglas fir under inert and oxidative environments" in Thermal Uses and Properties of Carbohydrates and Lignins, Edited by Shafizadeh, F., Sarkanen, K., and Tillman, D.A., 49-71, Academic Press.

Iglauer, N., and Bentley, F.F., (1974) "Pyrolysis GLC for the rapid identification of organic polymers", J. of Chromatog. Sci., 12, 23-33.

Lewellen, P.C., Peter, W.A. and Howard, J.B., (1977) "Cellulose pyrolysis kinetics and char formation mechanism", Sixteenth International Symp. on Combustion, 1471-1480.

Maa, P.S. and Bailie, R.C., (1978) "Experimental pyrolysis of cellulosic material", research paper presented at AIChE 84th National Meeting, Atlanta, February.

Martin, S., (1965) "Diffusion-controlled ignition of cellulosic materials by intense radiant energy", Proc. Tenth International Symposium on Combustion, 877-896.

Scott, D.S. and Piskorz, J., (1981) "Flash pyrolysis of biomass", fuels from biomass and wastes, Edited by Klass, D.L. and Emert, G.H., 421-434, Ann Arbor Science, Michigan.

Shafizadeh, F. and Bradbury, A.G.W., (1979) "Thermal degradation of cellulose in air and nitrogen at low temperatures", J. of Appl. Polym. Sci., 23, 1431-1442.

Shivadev, U.V. and Emmons, H.W., (1974) "Thermal degradation and spontaneous ignition of paper sheets in air by irradiation", Combustion and Flame, 22, 223-236.

Tsuchiya, Y. and Sumi, K., (1970) "Thermal decomposition products of cellulose", J. of Appl. Polym. Sci., 14, 2003-2013.

Tyler, R.J., (1979) "Flash pyrolysis of coals. 1. Devolatilization of a Victorian Brown coal in a small fluidized-bed reactor", Fuel, 58, 680-686.

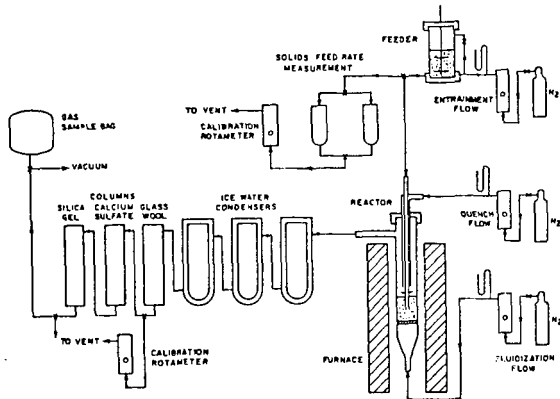


Figure 1 Micro Fluidized bed pyrolysis system (Scott and Piskorz, 1981)

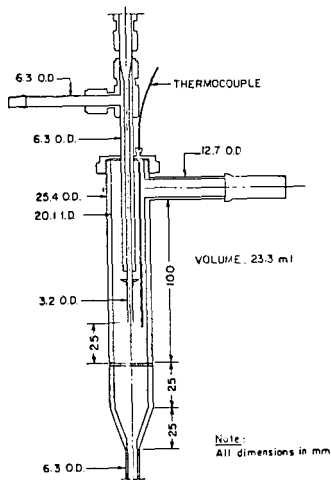


Figure 2 Construction details of fluidized bed (Scott and Piskorz, 1981)

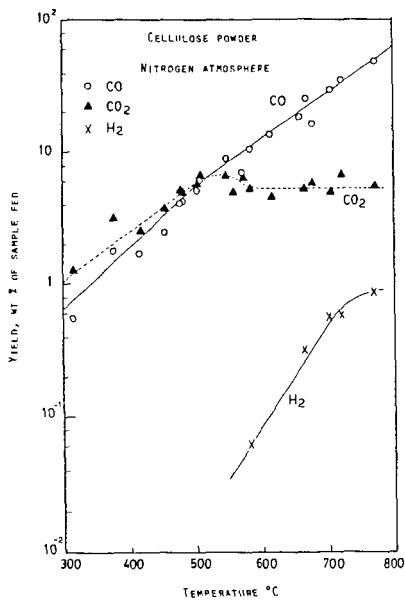


Figure 3 Light gas pyrolysis yield from MCP

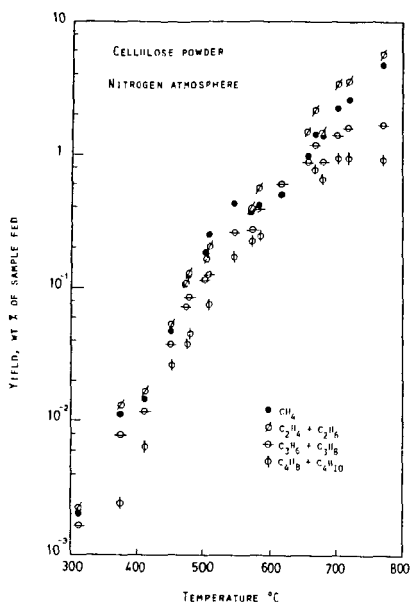


Figure 4 Yield of light hydrocarbon from MCP

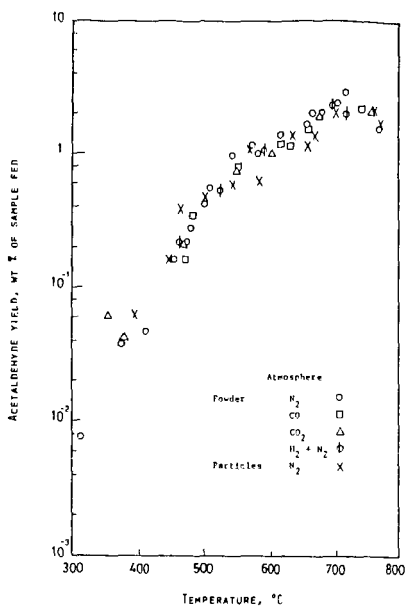


Figure 5 Yield of acetaldehyde from MCP and Cellulose particles

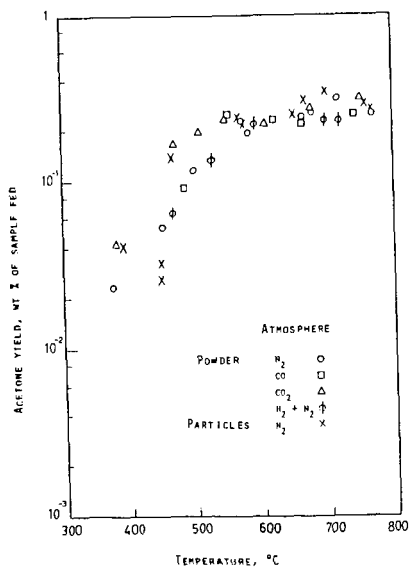


Figure 6 Yield of acetone from MCP and cellulose particles

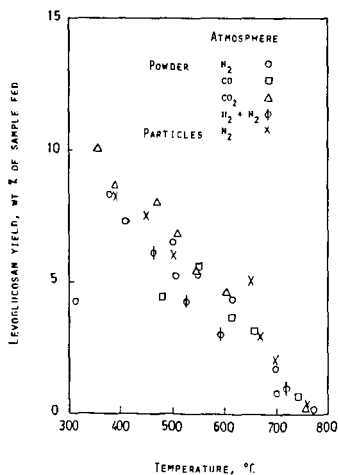


Figure 7 Yield of levoglucosan from MCP and cellulose particles

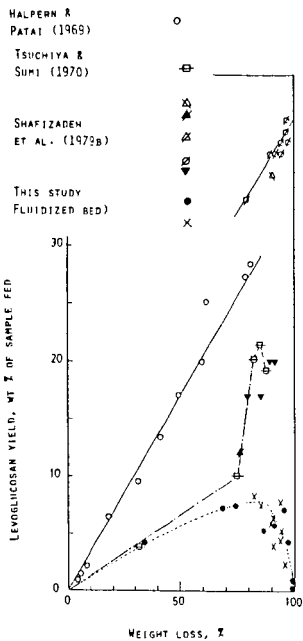


Figure 8 Levoglucosan yield as a function of weight loss with a comparison with slow pyrolysis data

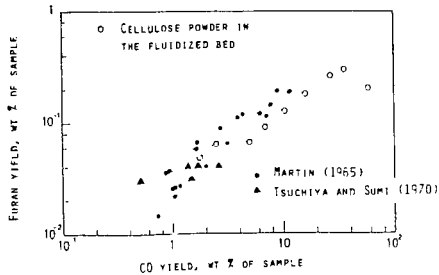


Figure 11 Cross plot of furan yields and CO yields from MCP

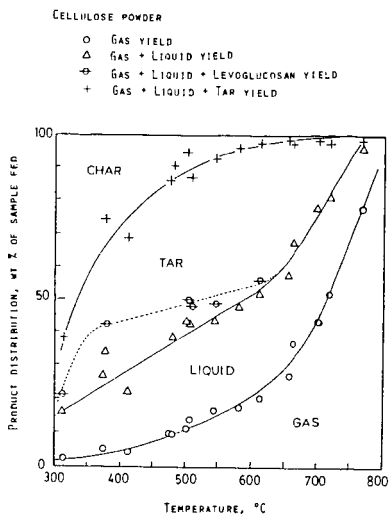


Figure 9 Product distribution in flash pyrolysis of MCP

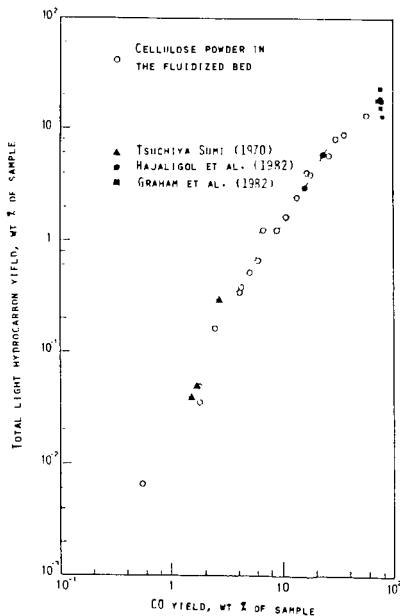


Figure 10 Cross plot of light hydrocarbon yields and CO yield from MCP

THE PREMIUM COAL SAMPLE PROGRAM AT THE ARGONNE NATIONAL LABORATORY

Karl S. Vorres
Chemistry Division, Bldg 211
Argonne National Laboratory
9700 South Cass Avenue
Argonne, Illinois 60439

PURPOSE OF THE PREMIUM COAL SAMPLE PROGRAM

The purpose of the Premium Coal Sample Program is to provide the coal science research community with long term supplies of a small number of premium coal samples that can be used as standards for comparison. The premium coal samples produced from each coal and distributed through this program will be as chemically and physically identical as possible, have well characterized chemical and physical properties, and will be stable over long periods of time. Coals will be mined, transported, processed into the desired particle and sample sizes, and packaged into environments as free of oxygen as possible. Humidity will also be controlled to keep the coals as pristine and in as stable of a condition as possible.

The need for a Premium Coal Sample Program was expressed at the Coal Sample Bank Workshop held March 27 and 28, 1981 in Atlanta, Georgia.

WHAT A PREMIUM SAMPLE IS

A premium coal sample has been specially selected, processed and stored to keep it as close to its original condition as possible. Specifically:

- Contact with oxygen has been minimized at all stages from mining, transport and processing in a nitrogen filled facility to sealing in amber colored glass vials.
- Relative humidity and temperature are controlled in the processing facility to maintain the equilibrium moisture of the original coal.
- Uniformity of samples is achieved by processing about 750 kg of coal in a single batch, mixing thoroughly in a special blender, and finishing with a spinning riffler to assure well-mixed samples. Activation analyses have confirmed the thoroughness of the mixing.
- Stability of the samples is maximized by sealing in amber-colored glass with a fuel-rich hydrogen-oxygen flame.
- Secure, long-term supplies result from an initial production of 10,000 five gram ampoules and 5,000 twenty gram ampoules with 50 five gallon sealed glass carboys in reserve for future ampoule production from each metric ton sample of coal.
- Some special needs can be met from lumps stored in argon in two reserve 55 gallon drums, and one 15 gallon drum as part of the original sample. A separate nitrogen filled glove box will be used for processing these requests.

SELECTION, MINING, AND TRANSPORT

Initially the coals have been selected to cover a wide range of degrees of coalification, mineral content, and sulfur content as well as commercial significance. The first three will be low-, medium- and high-volatile bituminous coals. The next two are planned to be lignite and sub-bituminous coals. These samples will be channel samples, representing a uniform cross section of the seam from top to bottom. Mining, under the supervision of coal geologists, involves removal of large lumps from a freshly exposed face to special plastic containers, transfer to stainless steel drums at the surface, purging with argon, transfer to refrigerated truck and immediate transport to the processing facility. A careful description of the geology of the sample area and location will be prepared and available as a referencable document.

SAMPLE PROCESSING

At the processing facility, a sample of argon from the coal drum will be analyzed to establish the relative humidity for the nitrogen filled processing facility. The stainless steel drums will be loaded into an airlock, which is then purged with nitrogen. The drums will be emptied into a crusher to reduce the size to 1/4", then pulverized in a cooled impact mill to obtain -20 mesh material. Coarse material will be recycled. The pulverized material will be collected in a nitrogen filled mixer-blender selected for gentle but thorough mixing. After thorough mixing the pulverized coal will be conveyed to a spinning riffler and sealed in 20 gram ampoules and 5 gallon glass carboys. The contents of some of the carboys will then be recycled to the pulverizer and crushed to pass a 100 mesh screen. After thorough blending this material will be conveyed to the packaging unit for sealing in 5 gram amber colored ampoules and 5 gallon borosilicate glass carboys. One of the goals of the Program is to complete the processing within seven days of exposing the mine face. Figure 1 indicates the coal storage system for a metric ton sample. Figure 2 is a block diagram of the coal sample preparation.

CHARACTERIZATION

The coals will be characterized by chemical and physical analysis. Results will be available for each coal in the form of a printed sample announcement. Requests to be placed on a mailing list should be sent to the author. The requestor should include mailing address, telephone number and research interests.

The analyses will include proximate, ultimate, calorific values, sulfur forms, equilibrium moisture, oxygen by neutron activation analysis, maceral analysis, Gieseler plasticity for the bituminous coals, and mineral matter major elements among others. Multiple laboratories will be involved in the analyses. Round robin analyses are also being organized.

A variety of stability monitoring tests will be used including evolved gas analysis. In addition the bituminous samples will be monitored by repetitive Gieseler plasticity analyses.

AVAILABILITY

Initial samples are expected to be available in fall, 1984. Samples will be made available to research personnel at a nominal replacement cost. A special glove box filled with nitrogen is available to transfer contents of ampoules to special sample holders on request. Also, a very limited quantity of lump coal, stored under similar inert conditions will be available on special request for special physical property measurements. The processing facility can be made available for occasional processing of special samples.

INFORMATION ON SAMPLES

Each recipient of samples is asked to provide either a literature reference to papers in widely circulated journals, or a copy of less widely circulated reports and papers, to be shared with other users of the samples. Listings of these references will be available on request to the author (phone 312-972-7374) either in printed versions or via computer terminal. The Premium Coal Sample Program expects to work with other coal sample programs in providing samples and sharing information.

Following the reports from the use of a number of samples, workshops are planned to facilitate sharing research results and to foster basic understanding of the chemistry and physical properties of the coal.

USERS ADVISORY COMMITTEE

A Users Advisory Committee provides useful suggestions to the Program Manager. This group includes: Dr. Blaine Cecil, U. S. Geological Survey; Dr. Marvin Poutsma, Oak Ridge National Laboratory; Dr. Ronald Pugmire, University of Utah; Dr. William Spackman, Pennsylvania State University; Dr. Irving Wender, University of Pittsburgh; Dr. Randall Winans, Argonne National Laboratory; Dr. John Young, Argonne National Laboratory.

ACKNOWLEDGEMENTS

The author gratefully acknowledges the support of the U. S. Department of Energy, Office of Basic Energy Sciences, Chemical Sciences Division.

Figure 1. Coal storage system.

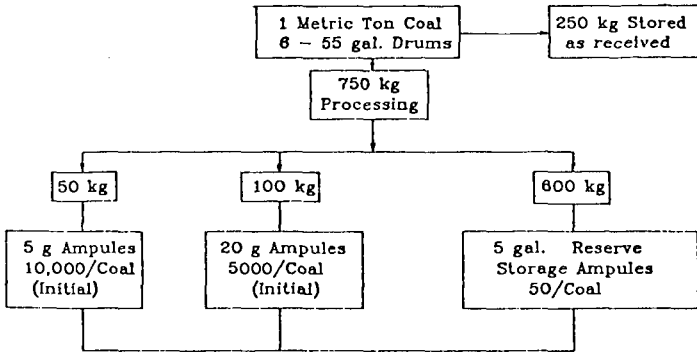


Figure 2. Coal Sample Preparation - Block Diagram

